Journal of Virology

Vesicular Stomatitis Virus Genomic RNA Persists *In Vivo* in the Absence of Viral Replication

Ian D. Simon, Nico van Rooijen and John K. Rose
J. Virol. **2010, 84(7):3280. DOI: 10.1128/JVI.02052-09.**
Published Ahead of Print 23 December 2009.

JOURNAL OF VIROLOGY, Apr. 2010, p. 3280–3286 Vol. 84, No. 7
0022-538X/10/$12.00 doi:10.1128/JVI.02052-09

Vesicular Stomatitis Virus Genomic RNA Persists *In Vivo* in the Absence of Viral Replication[▽]

Ian D. Simon,[1] Nico van Rooijen,[2] and John K. Rose[1]*

Department of Pathology, Yale University School of Medicine, New Haven, Connecticut 06510,[1] and Vrije Universiteit, VUMC, Department of Molecular Cell Biology, Faculty of Medicine, Van der Boechorststraat 7, 1081 BT Amsterdam, Netherlands[2]

Received 29 September 2009/Accepted 13 December 2009

Our previous studies using intranasal inoculation of mice with vesicular stomatitis virus (VSV) vaccine vectors showed persistence of vector genomic RNA (gRNA) for at least 60 days in lymph nodes in the absence of detectable infectious virus. Here we show high-level concentration of virus and gRNA in lymph nodes after intramuscular inoculation of mice with attenuated or single-cycle VSV vectors as well as long-term persistence of gRNA in the lymph nodes. To determine if the persistence of gRNA was due to ongoing viral replication, we developed a tagged-primer approach that was critical for detection of VSV mRNA specifically. Our results show that VSV gRNA persists long-term in the lymph nodes while VSV mRNA is present only transiently. Because VSV transcription is required for replication, our results indicate that persistence of gRNA does not result from continuing viral replication. We also performed macrophage depletion studies that are consistent with initial trapping of VSV gRNA largely in lymph node macrophages and subsequent persistence elsewhere in the lymph node.

Vesicular stomatitis virus (VSV) is a nonsegmented, negative-strand RNA virus and the prototype of the *Rhabdoviridae* family. VSV encodes 5 structural proteins: nucleocapsid protein (N), phosphoprotein (P), matrix protein (M), the surface glycoprotein (G), and the RNA-dependent RNA polymerase (L) (19). Live-attenuated vaccine vectors based on VSV have been developed and approved for clinical trials. Attenuated VSV-based vaccine vectors expressing foreign proteins induce potent immune responses and protect against viral and bacterial disease in several animal models, including nonhuman primates (9, 13, 15, 16, 17, 21, 25–27, 29, 30). A live-attenuated VSV-based Ebola virus vaccine vector has also been used in a person following a possible Ebola virus exposure (http://blogs.sciencemag.org/scienceinsider/2009/03/researchers-aro.html).

Highly attenuated and single-cycle VSV vectors have been extensively characterized previously in our laboratory and elsewhere (4, 17, 23, 24, 26). The highly attenuated live VSV vector VSV-CT1 has a truncation of the VSV G cytoplasmic domain from 29 amino acids to 1 amino acid (32). Compared to recombinant wild-type (rwt) vector (rwtVSV), the CT1 vector grows to approximately 20-fold-lower titers in tissue culture. The single-cycle VSV vector (VSVΔG) has a deletion of the VSV G gene but can be grown in complementing cells expressing the VSV G protein (33). This virus can infect cells and replicate for a single cycle but does not produce infectious progeny in the absence of complementing VSV G protein.

In previous studies, we found that VSV vaccine vector genomic RNA (gRNA) persists in the cervical draining lymph nodes for at least 60 days after intranasal (i.n.) inoculation with rwtVSV and VSV-CT1 vectors, although infectious virus could be recovered for only the first 4 days after inoculation (34). VSV-encoded antigen is also known to persist for at least 6 weeks after acute infection (35). Long-term persistence of live virus vector replication could present a safety concern. For example, in rare cases, measles virus replication can persist long-term and subsequent accumulation of mutations can lead to subacute sclerosing panencephalitis (2, 5, 31). The purpose of the current study was to determine if persistence of VSV gRNA was seen in lymph nodes following intramuscular (i.m.) inoculation and to examine the mechanism of persistence following i.m. or i.n. inoculation.

Our studies involved developing a quantitative, real-time, tagged-primer approach with complete specificity for VSV mRNA. This approach is used to overcome problems with lack of strand specificity caused by RNA self-priming during the reverse transcription (RT) step (6). Our studies show that VSV mRNA is present early after infection but does not persist, indicating that VSV replication is not ongoing.

Previous studies have demonstrated that macrophages trap VSV in lymphoid tissues such as the spleen and lymph node (3, 14, 20). Virus injected into the mouse footpad accumulates in $CD169^+$ $CD11b^+$ major histocompatibility complex (MHC) II^+ macrophages that comprise 1 to 2% of the mononuclear cells within the lymph node (14). Because $CD169^+$ macrophages are known to degrade VSV proteins and prevent viral dissemination (20), we examined the possibility that these might be the cells that trap and retain VSV gRNA long-term.

MATERIALS AND METHODS

Viruses and inoculum. Recombinant wild-type VSV (rwtVSV) and VSV-CT1 (114) were grown on BHK-21 cells (ATCC) in Dulbecco's modified Eagle's medium (DMEM) containing 5% fetal bovine serum (FBS) and penicillin-streptomycin (PS; 100 U/ml). VSVΔG was grown and titrated on BHK-G cells as previously described (33).

Inoculation of mice. Eight-week-old BALB/c mice were obtained from Charles River Laboratories and kept for at least 1 week prior to inoculation. Mice were housed in microisolator cages in a biosafety level 2-equipped animal facility. Immediately prior to inoculation, all recombinants were diluted in serum-free DMEM. For intranasal inoculation, mice were lightly anesthetized and inoculum containing 5×10^5 PFU was administered in 25 μl to the tip of the nose. For

* Corresponding author. Mailing address: Department of Pathology, Yale University School of Medicine, 310 Cedar St., LH 315, New Haven, CT 06520. Phone: (203) 785-6794. Fax: (203) 785-7467. E-mail: john.rose@yale.edu.

▽ Published ahead of print on 23 December 2009.

intramuscular inoculation, mice were injected in the right hind leg with 5×10^5 PFU in 50 μl. The Institutional Animal Care and Use Committee of Yale University approved of all animal experiments done in this study.

Recovery of infectious virus from tissue and plaque assay. Mice were euthanized via an anesthetic overdose. Lungs, spleens, and liver were harvested, rinsed in sterile phosphate-buffered saline (PBS), and placed in sterile, preweighed 2-ml Nunc cryotubes. Also, muscle from the hind legs and popliteal, inguinal, and iliac lymph nodes were collected and placed in cryotubes. Cervical lymph nodes along the dorsolateral side of the neck, specifically, the mandibular, accessory mandibular, and superficial parotid lymph nodes, were also collected and placed in Nunc cryotubes. The tissues were weighed in the tubes, dropped in liquid nitrogen, and later transferred to −80°C for storage. Organs were thawed on ice, suspended in 500 μl of DMEM containing 2.5% FBS and PS, and homogenized with Dounce homogenizers. Homogenates were centrifuged in an Eppendorf centrifuge for 3 min at 12,000 rpm, and the supernatants were frozen at −80°C. To determine viral titers, supernatants and plasma samples were thawed and plaque assays were performed as previously described (26).

Reverse transcription, real-time PCR assays. Copy numbers of gRNA from tissues were determined as described previously using standards of gRNA included with each experiment. (34). To determine VSV N mRNA copy number, an oligo(dT) column purified mRNA standard was prepared from an *in vitro* transcription reaction as previously described (28). The number of N transcripts in the sample was calculated using the N transcript molecular weight and the percentage of total VSV transcripts that correspond to N mRNA, as previously determined (11). Next, two-step reverse transcription-PCRs (RT-PCRs) were performed using the TaqMan reverse transcription reagent kit and Universal PCR Master Mix (Applied Biosystems). A standard curve for calculation of mRNA copy numbers was generated using reverse transcription reaction mixtures that contained 10^2, 10^3, 10^4, 10^5, 10^6, 10^7, or 10^8 copies of N mRNA and 1 μg carrier tRNA (VWR, West Chester, PA). This standard curve was included in every experiment.

RNA was isolated from tissue using the Qiagen RNeasy minikit (Valencia, CA), and 1 μg of RNA was reverse transcribed using the tagged primer (5′-ggcagtatcgtgaattcgatgcT_{19}CATAT-3′ [lowercase letters indicate the tag sequence]). To ensure that excess primer did not carry over to the PCR, RT products were treated with exonuclease I (2 U/sample) and incubated for 30 min at 37°C, followed by 15 min at 70°C. Real-time PCR was performed using the N forward primer (5′-CATGTCACTGCAAGGCCTAAGA-3′), tag reverse primer Rev (5′-GGCAGTATCGTGAATTCGATGC-3′), and the N probe (5′-6-carboxyfluorescein [FAM]-AGAAGACAATTGGCAAGTATGCTAAGTCAGAATTTG A-6-carboxytetramethylrhodamine [TAMRA]-3′) on an ABI 7500 real-time sequence detection system (Applied Biosystems). The number of copies of mRNA in each experimental sample was calculated from the threshold cycle values relative to the standard curve. The copy numbers are expressed as mRNA copy number per 10 mg of tissue.

Liposome-mediated elimination of macrophages *in vivo*. Mice were depleted of phagocytic macrophages using clodronate liposomes as described previously (7). Dichloromethylene-bisphosphonate (clodronate) was a gift of Roche Diagnostics GmbH, Mannheim, Germany, and was incorporated into liposomes as described previously (36). Mice were lightly anesthetized and then injected with 50 μl of clodronate liposomes or control PBS liposomes in the right hind footpad.

To verify macrophage depletion, popliteal, inguinal, and iliac lymph nodes were removed from 8-week-old BALB/c mice that had been treated with clodronate liposomes for 5 days. The nodes were cut into pieces, strained through nylon mesh, washed with PBS, and resuspended in blocking buffer. Macrophages were identified using conjugated antibodies specific for CD11b (BD Biosciences, San Jose, CA) and CD169 (AbD Serotec, Oxford, United Kingdom). Fluorescence intensities were measured with an LSRII flow cytometer, and the data were analyzed using FlowJo software (Tree Star, San Carlos, CA).

RESULTS

VSV vectors are confined to muscle and lymph nodes following intramuscular inoculation. To characterize the replication of VSV vaccine vectors *in vivo* following intramuscular (i.m.) inoculation, we determined the viral loads in hind leg muscle, popliteal lymph nodes (PLN), inguinal lymph nodes (ILN), iliac lymph nodes, plasma, spleen, lung, and liver at various times postinoculation. Only low and variable levels of infectious rwtVSV and VSV-CT1 were recovered from the muscle between 12 and 48 h postinoculation (h.p.i.) (Fig. 1A and C), and the total amount present in the muscle was less than 2% of the input virus. Infectious virus was no longer detectable in the muscle by 3 days postinoculation (d.p.i.). In addition, both viruses were recovered from the popliteal, inguinal, and iliac lymph nodes, which are the lymph nodes that drain the hind leg muscle. In the PLN, virus titers were highest at 12 h.p.i. and then fell to undetectable levels by 3 d.p.i. (Fig. 1B and D). Similar data were obtained for inguinal and iliac lymph nodes (not shown). No infectious virus was recovered from plasma or other peripheral organs or from lymph nodes on the left side of the animal, opposite the site of inoculation.

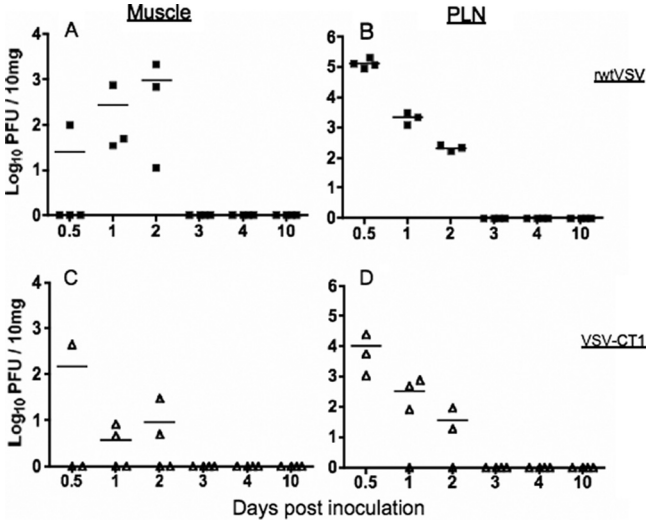

FIG. 1. Replication and spread of VSV vaccine vectors following i.m. inoculation. Eight-week-old BALB/c mice were inoculated i.m. with 5×10^5 PFU of rwtVSV (solid squares) or VSV-CT1 (open triangles). Viral titers were determined at the times indicated from the hind leg muscle (A and C) and popliteal lymph node (B and D) as described in Materials and Methods. Each point represents an individual animal. Each bar represents the mean value for all animals at that time point. The number of points indicates the number of animals (typically four) tested at each time.

To determine if any replication of virus was occurring in the animals, we calculated the total PFU recovered from all harvested organs (lungs; spleen; liver; hind leg muscle; popliteal, inguinal, and iliac lymph nodes; and cervical lymph nodes along the dorsolateral side of the neck) at 12 h or 24 h. Based on the average titers recovered, there appeared to be a small increase in the total amount of infectious virus relative to the input level for rwtVSV but not for VSV-CT1 (data not shown). However, these measurements had a very large standard deviation, and thus, we could not conclude that significant viral replication was occurring. Nevertheless, we could conclude that the spread of virus was contained to the lymph system (data not shown). This contrasts sharply with results obtained after intranasal inoculation, which leads to viremia and spread of virus to numerous organs, including lung, spleen, and liver as well as lymph nodes (34).

Genomic RNA levels reveal little viral replication following i.m. inoculation but long-term persistence of gRNA in lymph nodes. To examine the extent of replication of VSV vectors in greater detail, we used a reverse transcription, real-time PCR

TABLE 1. Input virus titers, gRNA levels, and recovered gRNA

Vector	Input PFU[a]	Input gRNA[b]	Recovered gRNA[c]	
			12 h	24 h
rwtVSV	5×10^5	6.5×10^9	$5.7 \times 10^9 \pm 3.2 \times 10^9$	$1.16 \times 10^{10} \pm 3.4 \times 10^9$
VSV-CT1	5×10^5	2.8×10^{10}	$1.5 \times 10^{10} \pm 4.0 \times 10^9$	$6.6 \times 10^9 \pm 1.14 \times 10^9$
VSVΔG	5×10^5	1.6×10^{11}	$1.2 \times 10^{10} \pm 3.5 \times 10^9$	$6.52 \times 10^9 \pm 2.4 \times 10^9$

[a] Number of PFU injected.
[b] Number of gRNA copies injected.
[c] Extrapolated total of gRNA copies recovered from all tissues harvested ± 1 standard deviation ($n = 3$ or 4).

assay (34) to detect and quantify VSV genomic RNA (gRNA) sequences. This assay also allowed us to detect the single-cycle vector VSVΔG, which does not produce infectious virus and, therefore, cannot be detected by plaque assay.

The total number of rwtVSV genomes present was less than the input level at 12 h.p.i. and only slightly higher than the input level at 24 h.p.i., suggesting little replication even for the rwt vector (Table 1). In contrast, the total VSV-CT1 and VSVΔG genome copy numbers were less than input copy numbers at both 12 h.p.i. and 24 h.p.i. (Table 1). Although the same virus titer was used for each inoculation, the ratio of input gRNA to PFU was much higher for the latter two vectors (Table 1), and thus, the higher input might obscure any possible increase due to replication.

The levels of gRNA from all three vectors were maximal in the muscle at 12 h.p.i., dropped approximately 100-fold by 3 d.p.i., and were mostly undetectable by day 10 (Fig. 2A, C, and E). Within the PLN (and other nodes examined; data not shown), the peak concentrations of gRNA were much higher, typically about 1×10^{10} copies/10 mg (Fig. 2B, D, and F), consistent with the higher viral titers found in lymph nodes. Between 12 h.p.i. and 3 d.p.i., gRNA levels dropped 100- to 1,000-fold in the PLN. gRNA was still detectable in the PLN, even at 60 d.p.i., for the VSV-CT1 and VSVΔG vectors but not for the rwt vector. Within the iliac and inguinal nodes VSVΔG gRNA levels from all mice were also above background at 60 d.p.i. (data not shown). The basis for this greater persistence of VSV-CT1 and VSVΔG gRNA is not known, but it could in part be due to the higher gRNA/PFU ratio in the CT1 and ΔG stocks than in the rwt stock (Table 1). Also, any cells infected with the VSVΔG virus would be expected to produce noninfectious particles that might be trafficked differently from infectious particles.

We also attempted to detect gRNA in blood and other peripheral organs. We were able to detect a transient appearance of a low level of gRNA from all three vectors in the spleen of about half of the animals, although we never detected infectious virus in plasma, lung, or liver.

A VSV N mRNA-specific real-time PCR assay to detect VSV replication. Previously, we have shown that VSV gRNA persists in the draining lymph nodes for at least 60 days after intranasal (i.n.) inoculation of rwtVSV and VSV-CT1 viruses (34). Similar persistence was seen here after i.m. inoculation. To determine if the persistence of gRNA was caused by a low level of ongoing replication or by retention of inactive gRNA sequences, we developed a quantitative VSV N mRNA-specific reverse transcription, real-time assay. If ongoing replication were occurring, it would require synthesis of N mRNA and protein (22), and therefore, this assay serves as a surrogate assay for VSV replication.

To eliminate problems of RNA self-priming that cause a lack of strand specificity, we adopted the tagged-primer approach that was first applied to specifically detect hepatitis C virus positive- and negative-strand RNAs (6). We generated a VSV N mRNA-specific primer tagged at its 5′ end with a nucleotide sequence unrelated to VSV (5′-ggcagtatcgtgaattcg atgcT_{20}CATAT-3′; unrelated sequence shown in lowercase). To generate a standard curve for quantification of N mRNA, this primer was used to prime cDNA synthesis from VSV N

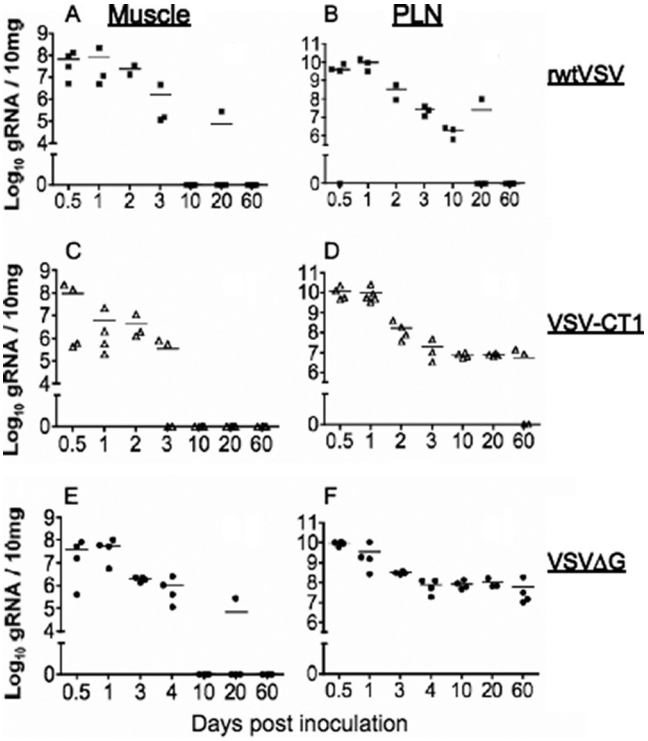

FIG. 2. Persistence of VSV gRNA following i.m. inoculation. Eight-week-old BALB/c mice were inoculated with 5×10^5 PFU of rwtVSV (solid squares) (A and B), VSV-CT1 (open triangles) (C and D), and VSVΔG (solid circles) (E and F). Leg muscle and popliteal lymph nodes (PLN) were harvested at the indicated times postinoculation. RNA was isolated from the tissue, and a reverse transcription, real-time PCR assay was performed to quantify gRNA. Each point represents the result from an individual animal. Copy numbers below 1×10^4 copies (background of the assay) are all indicated arbitrarily as 10^0. Each bar represents the mean value for all animals at that time point.

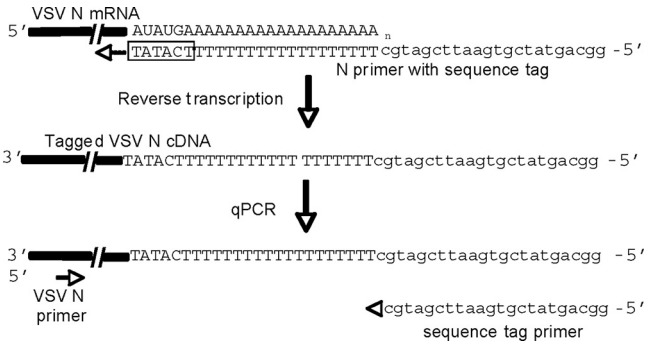

FIG. 3. Diagram of tagged-primer assay specific for positive-strand VSV N mRNA. The first 5 nucleotides at the 3′ end of the tagged primer (boxed) are complementary to the VSV N mRNA just preceding the poly(A) tail and not to other VSV mRNAs. The lowercase sequence following the T_{19} tract is the unrelated sequence tag. cDNA generated with this primer is then amplified with a VSV N internal primer, a primer corresponding only to the tag sequence, and a labeled probe, as described in Materials and Methods.

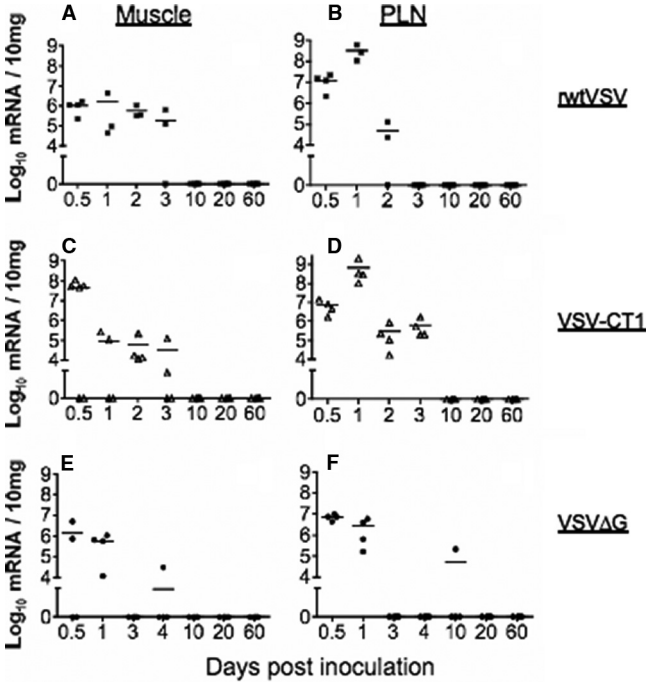

FIG. 4. Lack of persistence of VSV N mRNA following i.m. inoculation. Eight-week-old BALB/c mice were inoculated with 5×10^5 PFU of rwtVSV (solid squares) (A and B), VSV-CT1 (open triangles) (C and D), or VSVΔG (solid circles) (E and F). Leg muscle and popliteal lymph nodes (PLN) were harvested at the indicated times postinoculation, RNA was prepared from the tissues, and N mRNA was quantified using the tagged-primer method. The graph shows the number of mRNA copies per 10 mg of tissue, with each point representing an individual animal. Copy numbers below 1×10^4 copies (background of the assay) are all indicated arbitrarily as 10^0. Bars represent the mean values.

mRNA made *in vitro* (11). The real-time PCR was then carried out using a VSV N-specific primer (forward) and a primer corresponding exactly to the tag sequence. This procedure ensures that only cDNA generated from the tagged primer is amplified in this step and eliminates amplification of DNA made by RNA self-priming (Fig. 3). The assay was specific for positive-strand (VSV N mRNA) sequences, as it gave no background signal even after reverse transcription and 50 cycles of amplification using high levels (10^8 copies) of purified negative-strand gRNA template. In contrast, when we used purified gRNA and either no DNA primer or an untagged 5′-T_{20}CATAT primer in the reverse transcription reaction followed by real-time PCR using two internal N primers, there was a high-level false-positive signal for VSV mRNA.

VSV transcription is not detected later than 3 to 10 days after i.m. inoculation. We next used the mRNA-specific assay to determine how long VSV transcription persisted after i.m. inoculation with VSV vectors. Within the muscle, VSV N mRNA levels for all three vectors peaked at 12 h.p.i. (Fig. 4A, C, and E). For rwtVSV and VSVΔG, these levels were generally lower than the level of genomic RNA detected at this time, probably reflecting the high level of input genomes derived from noninfectious VSV particles (Table 1). In contrast, VSV-CT1 mRNA levels at 12 h.p.i. are much higher than those of the other two vectors (Fig. 4C). Yet, the N mRNA transcripts from all VSV vectors were undetectable in the leg muscle between 3 and 10 d.p.i. (Fig. 4A, C, and E).

For all three vectors, approximately 10^7 N mRNA copies/10 mg were found in the PLN at 12 h.p.i. (Fig. 4B, D, and F). These levels increased for both rwt and CT1 vectors over the next 12 h, while VSVΔG N mRNA levels remained constant or dropped. N mRNA transcripts from rwtVSV were not detectable by 3 d.p.i., and VSV-CT1 mRNA sequences were undetectable by 10 d.p.i. VSVΔG transcripts were also undetectable in the PLN by 3 d.p.i. Similar data were obtained from inguinal and iliac lymph nodes (not shown). Thus, the kinetics of clearance of VSV mRNA was relatively rapid, similar to the clearance of infectious virus and far more rapid than clearance of gRNA. These results indicate that the persistence of gRNA is not due to ongoing viral replication but rather to trapping of gRNA.

Lack of persistence of VSV N mRNA after intranasal inoculation. In our earlier studies of VSV vector replication and spread following i.n. inoculation, we found long-term persistence (>60 days) of VSV gRNA from rwtVSV, VSV-CT1, and VSVΔG in the cervical lymph nodes but not in the lungs. To examine persistence of VSV transcription in mice inoculated by this route, the lungs and cervical lymph nodes were harvested at various times postinoculation with the three vectors. For rwtVSV, we found peak levels of about 1×10^8 N mRNA copies/10 mg in the lungs and 2×10^9 N mRNA copies/10 mg within the lymph nodes (Fig. 5A and B). However, VSV N mRNA was undetectable in the majority of animals by day 20 and was undetectable in all animals by day 60. N mRNA sequences from both CT1 and ΔG vectors were initially present in lung and lymph nodes, but they also became undetectable between 10 and 20 d.p.i. (data not shown). Thus, even after i.n. inoculation, where VSV replication and spread are more vigorous, there is no evidence for long-term persistence of VSV replication.

Role of lymph node macrophages in trapping and persistence of VSV gRNA. Recent studies have shown that $CD169^+$ sinusoidal macrophages in the mouse PLN can efficiently trap VSV particles that are injected into the footpad (14). To ex-

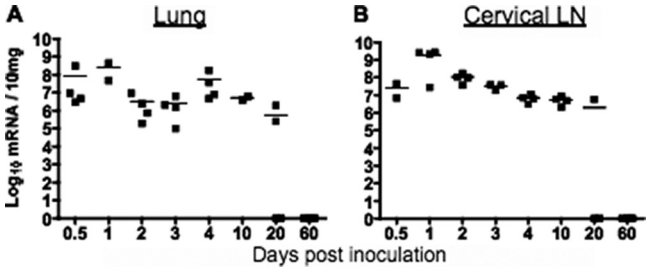

FIG. 5. Lack of persistence of VSV N mRNA following i.n. inoculation. Eight-week-old BALB/c mice were inoculated with 5×10^5 PFU of rwtVSV. Lungs (A) and cervical lymph nodes (LN) (B) were harvested at various times postinoculation, RNA was prepared from the tissues, and N mRNA was quantified using the tagged-primer method. The graph shows the number of mRNA copies per 10 mg of tissue, with each point representing values determined from an individual animal. Copy numbers below 1×10^4 copies (background of the assay) are all indicated arbitrarily as 10^0. Bars represents the mean values.

amine the role that macrophages might play in retention and persistence of VSV gRNA in the PLN following i.m. inoculation, macrophages were depleted from the PLN by injection of clodronate liposomes into the footpad (8). As shown in Fig. 6A, the depletion of the $CD11b^+$ $CD169^+$ macrophages was >98% effective.

Depleted and control mice were inoculated i.m. with rwtVSV and sacrificed at 6 h postinoculation, and VSV gRNA copy numbers in the PLN were determined (Fig. 6B and C). The data showed a significant decrease of about 10-fold ($P < 0.007$, two-tailed unpaired t test) in the gRNA levels as a result of the depletion (Fig. 6B). Because the macrophage depletion was greater than 98% effective, the 10-fold reduction in gRNA at 6 h.p.i. suggests that macrophages were the major, but probably not the only, cells trapping VSV gRNA at 6 h.p.i. This result is in agreement with previous studies employing footpad injection of VSV where titers of virus recovered from the PLN were reduced 10-fold in depleted animals compared to control animals (14).

To determine if macrophages were responsible for longer-term retention of VSV gRNA, we performed depletions on animals at 5 d.p.i. with VSV vectors and then measured gRNA levels at 10 d.p.i. when depletion was complete. Although there was a decrease in the average gRNA levels for both rwtVSV and VSVΔG vector levels following depletion (Fig. 6C and D), there was also a wide range in the values among the animals, and the differences were not statistically significant.

To investigate persistence at even later times, mice were inoculated with VSVΔG, depleted of macrophages at 50 d.p.i., and then tested for gRNA levels at 60 d.p.i. This experiment was performed only on animals infected with the VSVΔG virus because this vector gave consistently high levels of gRNA retention at 60 d.p.i. in the PLN (Fig. 2). The results (Fig. 6E) did not show a significant decrease in gRNA levels following depletion, indicating that macrophages are not the major reservoirs of VSVΔG gRNA at late times. We also verified that the macrophages were still absent at 10 days after depletion (data not shown).

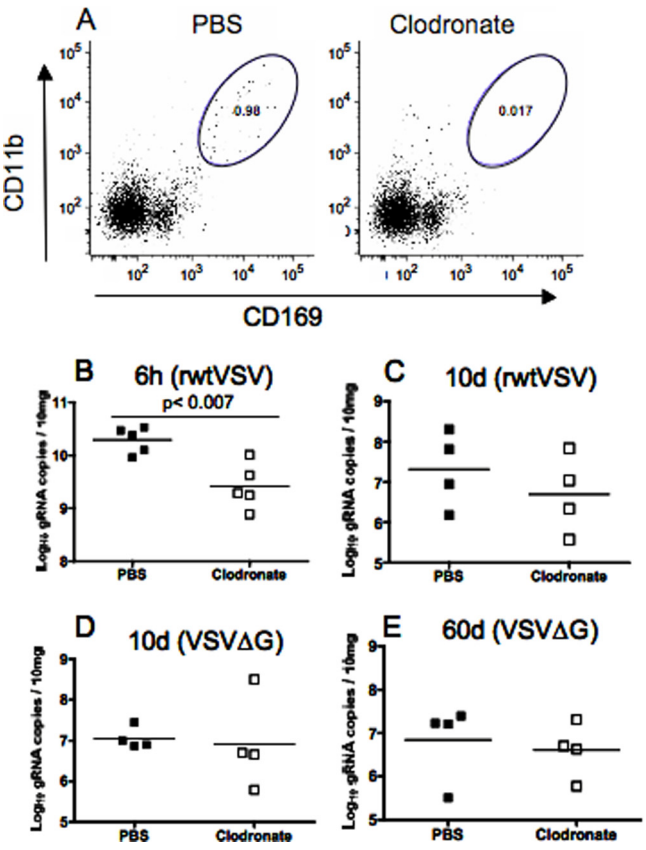

FIG. 6. Effects of lymph node macrophage depletion on trapping of gRNA. (A) Representative flow cytometry plots of PLN cells stained with anti-CD11b and anti-CD169 at 5 days following injection of control PBS liposomes or clodronate liposomes into the footpad. The numbers circled are the percentages of cells that were $CD11b^+$ $CD169^+$ in the PLN. (B) VSV gRNA levels in the PLN of control or macrophage-depleted mice at 6 h after i.m. injection with 3.5×10^7 PFU of rwtVSV. Depletions were performed 5 days prior to injection. (C and D) VSV gRNA levels in the PLN of mice that were inoculated i.m. with 3.5×10^7 PFU of rwtVSV (C) or VSVΔG (D). Five days after inoculation, PLN macrophages were depleted with clodronate liposomes, and the levels of gRNA in the PLN of control or depleted mice were measured 5 days later (10 d.p.i.). (E) VSV gRNA levels in the PLN of mice that were inoculated i.m. with 3.5×10^7 PFU of VSVΔG. Fifty days after inoculation, PLN macrophages were depleted with clodronate liposomes, and the levels of gRNA in the PLN of control or depleted mice were measured 10 days later (60 d.p.i.). Control experiments showed that macrophage depletion was still complete at 10 days after clodronate treatment. Each point represents the gRNA level determined from an individual animal. Bars represent the mean values.

DISCUSSION

Live-attenuated and single-cycle VSV-based experimental vaccine vectors have been used extensively to generate robust immune responses in a variety of species. In previous studies, we showed extensive replication and spread of rwtVSV and attenuated vectors to multiple organs following intranasal inoculation, while the single-cycle vectors were very limited in spread. The extent of spread correlated directly with the ability of the vectors to induce immune responses when given by this route (23). In addition, we reported long-term persistence of vector gRNA in lymph nodes.

In the current study focusing on i.m. inoculation, we determined that the rwtVSV, replication-attenuated, and single-cycle VSV vectors were all trafficked efficiently from the site of injection in the muscle to lymph nodes but were not propagated to other tissues. Our finding of similar peak levels of gRNA in the lymph nodes for all vectors likely explains the ability of the attenuated and single-cycle vectors to generate immune responses comparable to those for rwtVSV vectors when given by this route (23). The efficient trafficking of the single-cycle vector to the lymph node indicates that production of new infectious virus and subsequent rounds of infection are not required for this trafficking. Our results are consistent with a recent study showing that VSV particles made replication defective with UV light are efficiently trafficked to and trapped in lymph nodes after injection into the mouse footpad (14).

VSV vectors do not replicate extensively in the muscle tissue and are most likely carried through the lymphatics and concentrated in the draining lymph nodes where effective antigen presentation and stimulation of immune responses occur. Our data indicate also that little replication of VSV occurred in the lymph nodes because the total gRNA recovered from the nodes was similar to the input gRNA level.

We have previously seen long-term persistence of VSV gRNA within draining lymph nodes after i.n. inoculation (34). Long-term persistence of VSV RNA in cattle and hamsters has also been reported elsewhere (1, 18). A recent study has also reported the concentration in lymph nodes and long-term persistence of rwt and other attenuated VSV vector RNAs after i.m. inoculation of mice (12).

The most interesting question related to the persistence of vector gRNA is the mechanism. We suggested previously that the gRNA persistence could be due either to low-level, long-term VSV replication that is refractory to clearance by the immune system or to sequestration of inactive gRNA sequences (34). Long-term persistence of VSV-encoded antigen has also been reported elsewhere (35), but the mechanism of antigen persistence is not known. Because we found persistence of gRNA even in mice infected with the single-cycle, VSVΔG vector, we could exclude any requirement for multiple rounds of infection to maintain persistence. We believe that persistence of VSV-encoded antigen for 6 weeks (35) is probably occurring in the absence of VSV replication. Nonetheless, we could not exclude the possibility that VSVΔG vectors might be able to replicate long-term in some cells without causing cell death.

To determine definitively if VSV replication was persistent, we developed a VSV mRNA assay specific for the most abundant VSV mRNA encoding the VSV N protein. VSV replication requires continuing VSV mRNA and protein synthesis, and thus, the absence of mRNA would indicate absence of replication (22). Similar to gRNA, we found that VSV N mRNA transcripts appeared soon after infection in the animals. But, unlike gRNA, VSV N mRNA did not persist beyond 4 to 10 days postinfection after i.m. inoculation or beyond 20 d.p.i. following i.n. inoculation. The levels of mRNA detected were less than the levels of gRNA, probably indicating that few of the gRNA molecules were involved in transcription and replication and thus were likely derived from noninfectious input virions. Our data indicate that the gRNA detected over the long term is not involved in replication and is probably sequestered somewhere in the lymph node, perhaps in the form of RNase-resistant nucleocapsids. The lack of detectable long-term VSV vaccine vector replication *in vivo* minimizes concerns about accumulation of mutations in live-attenuated vectors that could potentially lead to increased vector virulence.

The elegant studies by Junt et al. have shown that $CD169^+$ lymph node macrophages are critical for binding and trapping of VSV virions (14). Furthermore, translocation of VSV antigen to B and T cells occurs shortly after entering the lymph node (10, 14). Our results using macrophage depletion from lymph nodes are consistent with initial trapping of VSV gRNA by $CD169^+$ lymph node macrophages but indicate that the majority of the long-term persistence of VSV gRNA in lymph nodes is not occurring in these cells.

ACKNOWLEDGMENTS

We thank Brett Lindenbach for suggesting the use of the tagged-primer approach for specific detection of VSV mRNA and members of the Rose laboratory for helpful suggestions on the manuscript.

This work was supported by NIH grant R37AI45357.

REFERENCES

1. **Barrera, J. C., and G. J. Letchworth.** 1996. Persistence of vesicular stomatitis virus New Jersey RNA in convalescent hamsters. Virology **219:**453–464.
2. **Cattaneo, R., A. Schmid, M. A. Billeter, R. D. Sheppard, and S. A. Udem.** 1988. Multiple viral mutations rather than host factors cause defective measles virus gene expression in a subacute sclerosing panencephalitis cell line. J. Virol. **62:**1388–1397.
3. **Ciavarra, R. P., K. Buhrer, N. Van Rooijen, and B. Tedeschi.** 1997. T cell priming against vesicular stomatitis virus analyzed in situ: red pulp macrophages, but neither marginal metallophilic nor marginal zone macrophages, are required for priming CD4+ and CD8+ T cells. J. Immunol. **158:**1749–1755.
4. **Clarke, D. K., F. Nasar, M. Lee, J. E. Johnson, K. Wright, P. Calderon, M. Guo, R. Natuk, D. Cooper, R. M. Hendry, and S. A. Udem.** 2007. Synergistic attenuation of vesicular stomatitis virus by combination of specific G gene truncations and N gene translocations. J. Virol. **81:**2056–2064.
5. **Connolly, J. H., I. V. Allen, L. J. Hurwitz, and J. H. Millar.** 1967. Measles-virus antibody and antigen in subacute sclerosing panencephalitis. Lancet **i:**542–544.
6. **Craggs, J. K., J. K. Ball, B. J. Thomson, W. L. Irving, and A. M. Grabowska.** 2001. Development of a strand-specific RT-PCR based assay to detect the replicative form of hepatitis C virus RNA. J. Virol. Methods **94:**111–120.
7. **Delemarre, F. G., N. Kors, G. Kraal, and N. van Rooijen.** 1990. Repopulation of macrophages in popliteal lymph nodes of mice after liposome-mediated depletion. J. Leukoc. Biol. **47:**251–257.
8. **Delemarre, F. G., N. Kors, and N. van Rooijen.** 1990. Elimination of spleen and of lymph node macrophages and its difference in the effect on the immune response to particulate antigens. Immunobiology **182:**70–78.
9. **Egan, M. A., S. Y. Chong, N. F. Rose, S. Megati, K. J. Lopez, E. B. Schadeck, J. E. Johnson, A. Masood, P. Piacente, R. E. Druilhet, P. W. Barras, D. L. Hasselschwert, P. Reilly, E. M. Mishkin, D. C. Montefiori, M. G. Lewis, D. K. Clarke, R. M. Hendry, P. A. Marx, J. H. Eldridge, S. A. Udem, Z. R. Israel, and J. K. Rose.** 2004. Immunogenicity of attenuated vesicular stomatitis virus vectors expressing HIV type 1 Env and SIV Gag proteins: comparison of intranasal and intramuscular vaccination routes. AIDS Res. Hum. Retrovir. **20:**989–1004.
10. **Hickman, H. D., K. Takeda, C. N. Skon, F. R. Murray, S. E. Hensley, J. Loomis, G. N. Barber, J. R. Bennink, and J. W. Yewdell.** 2008. Direct priming of antiviral CD8+ T cells in the peripheral interfollicular region of lymph nodes. Nat. Immunol. **9:**155–165.
11. **Iverson, L. E., and J. K. Rose.** 1981. Localized attenuation and discontinuous synthesis during vesicular stomatitis virus transcription. Cell **23:**477–484.
12. **Johnson, J. E., J. W. Coleman, N. K. Kalyan, P. Calderon, K. J. Wright, J. Obregon, E. Ogin-Wilson, R. J. Natuk, D. K. Clarke, S. A. Udem, D. Cooper, and R. M. Hendry.** 2009. In vivo biodistribution of a highly attenuated recombinant vesicular stomatitis virus expressing HIV-1 Gag following intramuscular, intranasal, or intravenous inoculation. Vaccine **27:**2930–2939.
13. **Jones, S. M., H. Feldmann, U. Stroher, J. B. Geisbert, L. Fernando, A. Grolla, H. D. Klenk, N. J. Sullivan, V. E. Volchkov, E. A. Fritz, K. M. Daddario, L. E. Hensley, P. B. Jahrling, and T. W. Geisbert.** 2005. Live attenuated recombinant vaccine protects nonhuman primates against Ebola and Marburg viruses. Nat. Med. **11:**786–790.

14. **Junt, T., E. A. Moseman, M. Iannacone, S. Massberg, P. A. Lang, M. Boes, K. Fink, S. E. Henrickson, D. M. Shayakhmetov, N. C. Di Paolo, N. van Rooijen, T. R. Mempel, S. P. Whelan, and U. H. von Andrian.** 2007. Subcapsular sinus macrophages in lymph nodes clear lymph-borne viruses and present them to antiviral B cells. Nature **450:**110–114.
15. **Kahn, J. S., A. Roberts, C. Weibel, L. Buonocore, and J. K. Rose.** 2001. Replication-competent or attenuated, nonpropagating vesicular stomatitis viruses expressing respiratory syncytial virus (RSV) antigens protect mice against RSV challenge. J. Virol. **75:**11079–11087.
16. **Kapadia, S. U., J. K. Rose, E. Lamirande, L. Vogel, K. Subbarao, and A. Roberts.** 2005. Long-term protection from SARS coronavirus infection conferred by a single immunization with an attenuated VSV-based vaccine. Virology **340:**174–182.
17. **Kapadia, S. U., I. D. Simon, and J. K. Rose.** 2008. SARS vaccine based on a replication-defective recombinant vesicular stomatitis virus is more potent than one based on a replication-competent vector. Virology **376:**165–172.
18. **Letchworth, G. J., J. C. Barrera, J. R. Fishel, and L. Rodriguez.** 1996. Vesicular stomatitis New Jersey virus RNA persists in cattle following convalescence. Virology **219:**480–484.
19. **Lyles, D. S., and C. E. Rupprecht.** 2007. Rhabdoviridae, p. 1363–1408. *In* D. M. Knipe, P. M. Howley, D. E. Griffin, R. A. Lamb, M. A. Martin, B. Roizman, and S. E. Straus (ed.), Fields virology, 5th ed., vol. 1. Lippincott Williams & Wilkins, Philadelphia, PA.
20. **Oehen, S., B. Odermatt, U. Karrer, H. Hengartner, R. Zinkernagel, and C. Lopez-Macias.** 2002. Marginal zone macrophages and immune responses against viruses. J. Immunol. **169:**1453–1458.
21. **Palin, A., A. Chattopadhyay, S. Park, G. Delmas, R. Suresh, S. Senina, D. S. Perlin, and J. K. Rose.** 2007. An optimized vaccine vector based on recombinant vesicular stomatitis virus gives high-level, long-term protection against Yersinia pestis challenge. Vaccine **25:**741–750.
22. **Perlman, S. M., and A. S. Huang.** 1973. RNA synthesis of vesicular stomatitis virus. V. Interactions between transcription and replication. J. Virol. **12:** 1395–1400.
23. **Publicover, J., E. Ramsburg, and J. K. Rose.** 2005. A single-cycle vaccine vector based on vesicular stomatitis virus can induce immune responses comparable to those generated by a replication-competent vector. J. Virol. **79:**13231–13238.
24. **Publicover, J., E. Ramsburg, and J. K. Rose.** 2004. Characterization of nonpathogenic, live, viral vaccine vectors inducing potent cellular immune responses. J. Virol. **78:**9317–9324.
25. **Reuter, J. D., B. E. Vivas-Gonzalez, D. Gomez, J. H. Wilson, J. L. Brandsma, H. L. Greenstone, J. K. Rose, and A. Roberts.** 2002. Intranasal vaccination with a recombinant vesicular stomatitis virus expressing cottontail rabbit papillomavirus L1 protein provides complete protection against papillomavirus-induced disease. J. Virol. **76:**8900–8909.
26. **Roberts, A., L. Buonocore, R. Price, J. Forman, and J. K. Rose.** 1999. Attenuated vesicular stomatitis viruses as vaccine vectors. J. Virol. **73:**3723–3732.
27. **Roberts, A., E. Kretzschmar, A. S. Perkins, J. Forman, R. Price, L. Buonocore, Y. Kawaoka, and J. K. Rose.** 1998. Vaccination with a recombinant vesicular stomatitis virus expressing an influenza virus hemagglutinin provides complete protection from influenza virus challenge. J. Virol. **72:**4704–4711.
28. **Rose, J. K., H. F. Lodish, and M. L. Brock.** 1977. Giant heterogeneous polyadenylic acid on vesicular stomatitis virus mRNA synthesized in vitro in the presence of S-adenosylhomocysteine. J. Virol. **21:**683–693.
29. **Rose, N. F., P. A. Marx, A. Luckay, D. F. Nixon, W. J. Moretto, S. M. Donahoe, D. Montefiori, A. Roberts, L. Buonocore, and J. K. Rose.** 2001. An effective AIDS vaccine based on live attenuated vesicular stomatitis virus recombinants. Cell **106:**539–549.
30. **Schlereth, B., J. K. Rose, L. Buonocore, V. ter Meulen, and S. Niewiesk.** 2000. Successful vaccine-induced seroconversion by single-dose immunization in the presence of measles virus-specific maternal antibodies. J. Virol. **74:**4652–4657.
31. **Schmid, A., P. Spielhofer, R. Cattaneo, K. Baczko, V. ter Meulen, and M. A. Billeter.** 1992. Subacute sclerosing panencephalitis is typically characterized by alterations in the fusion protein cytoplasmic domain of the persisting measles virus. Virology **188:**910–915.
32. **Schnell, M. J., L. Buonocore, E. Boritz, H. P. Ghosh, R. Chernish, and J. K. Rose.** 1998. Requirement for a non-specific glycoprotein cytoplasmic domain sequence to drive efficient budding of vesicular stomatitis virus. EMBO J. **17:**1289–1296.
33. **Schnell, M. J., J. E. Johnson, L. Buonocore, and J. K. Rose.** 1997. Construction of a novel virus that targets HIV-1-infected cells and controls HIV-1 infection. Cell **90:**849–857.
34. **Simon, I. D., J. Publicover, and J. K. Rose.** 2007. Replication and propagation of attenuated vesicular stomatitis virus vectors in vivo: vector spread correlates with induction of immune responses and persistence of genomic RNA. J. Virol. **81:**2078–2082.
35. **Turner, D. L., L. S. Cauley, K. M. Khanna, and L. Lefrancois.** 2007. Persistent antigen presentation after acute vesicular stomatitis virus infection. J. Virol. **81:**2039–2046.
36. **Van Rooijen, N., and A. Sanders.** 1994. Liposome mediated depletion of macrophages: mechanism of action, preparation of liposomes and applications. J. Immunol. Methods **174:**83–93.